Ex vivo expression of chemokine receptors on cells surrounding cutaneous nerves in patients with HIV-associated sensory neuropathy

Jenjira MOUNTFORD[a], Fitri OCTAVIANA[b], Riwanti ESTIASARI[b], Denise DEWANTO SETIAWAN[b], Ibnu ARIYANTO[c], Silvia LEE[a,d], Jessica GAFF[a], Constance CHEW[e], Connie JACKAMAN[a], Peter KAMERMAN[a,f], Catherine CHERRY[f,g,h], Patricia PRICE[a,c,f]

[a] School of Biomedical Sciences, Curtin University, Bentley, Australia

[b]Neurology Department, Faculty of Medicine, University of Indonesia, Jakarta, Indonesia

[c]Virology and Cancer Pathobiology Research Center, Universitas Indonesia, Jakarta, Indonesia

[d]Department of Microbiology, Royal Perth Hospital, Perth, Australia

[e]Pathology and Laboratory Medicine, University of Western Australia, Perth, Australia

[f]School of Physiology, Faculty of Health Sciences, University of the Witwatersrand, Johannesburg, South Africa

[g]Department of Infectious Diseases, Alfred Health and Monash University, Melbourne, Australia

[h]Burnet Institute, Melbourne, Australia

Corresponding Author:

A/Professor Patricia Price

School of Biomedical Science, Curtin University, Bentley, Australia

Tel: 618-92669716

Email: patricia.price@curtin.edu.au

Short Title: *Chemokine receptors and HIV neuropathy*

Words: 3466

Abstract

Objective: HIV-associated sensory neuropathy (HIV-SN) remains common in HIV+ individuals receiving anti-retroviral therapy (ART), even though neurotoxic anti-retroviral drugs (e.g. stavudine) have been phased out of use. Accumulating evidence indicates that the neuropathy is immune-mediated. We hypothesise that chemokines produced locally in the skin promote migration of macrophages and T-cells into the tissue, damaging cutaneous nerves causing HIV-SN.

Design: We assessed chemokine receptor expression on infiltrating CD14+ and CD3+ cells around cutaneous nerves in standardised skin biopsies from HIV-SN+ patients (*n*=5), HIV-SN-patients (*n*=9) and healthy controls (*n*=4).

Methods: The AIDS Clinical Trials Group Brief Peripheral Neuropathy Screen was used to assess Indonesian HIV+ patients receiving ART without stavudine (case definition: bilateral presence of at least one symptom and at least one sign of neuropathy). Distal leg skin biopsies were stained to visualise chemokine receptors; CCR2, CCR5, CXCR3, CXCR4, CX3CR1, infiltrating CD3+ and CD14+ cells and protein-gene-product 9.5 on nerves, using immunohistochemistry and 4-colour confocal microscopy.

Results: Intraepidermal nerve fibre density was variable in patients without HIV-SN and generally lower in those with HIV-SN. CX3CR1 was more evident on CD14+ cells whereas CCR2, CCR5, CXCR3 and CXCR4 were more common on CD3+ cells. Expression of CX3CR1, CCR2 and CCR5 was more common in HIV-SN+ patients than those without HIV-SN. CXCR3 and CXCR4 were upregulated in all HIV+ patients, compared with healthy controls.

Conclusion: Inflammatory macrophages expressing CX3CR1 and T-cells expressing CCR2 and CCR5 may participate in peripheral nerve damage leading to HIV-SN in HIV+ patients treated without stavudine. Further characterisation of these cells is warranted. (*250 words*).

Introduction

HIV-associated sensory neuropathy (HIV-SN) is a common neurologic manifestation of HIV and its treatment. Historically, neuropathy has been described in about 30% of treatment-naïve patients with advanced HIV disease [1, 2], and about 60% of patients on anti-retroviral therapy (ART) regimens that included zalcitabine, didanosine or stavudine [3, 4]. It is now accepted that these drugs are neurotoxic. Despite patients now starting treatment earlier and without known neurotoxic antiretroviral agents, HIV-SN remains a problem [5-7].

A pathological hallmark of HIV-SN is distal degeneration of long axons in a "dying back" pattern, which is associated with reduced intraepidermal nerve fibre density (IENFD), nerve fibre swelling, and mononuclear cell infiltration [8, 9]. HIV-infected and uninfected activated macrophages can infiltrate peripheral nerves, dorsal root ganglia (DRG) [10] and/or tissues adjacent to peripheral nerves, and release cytokines such as Tumour Necrosis Factor alpha (TNF-α), Interferon-gamma (IFN-γ) and Interleukin (IL)-1 and/or IL-17, which can cause axonal degeneration [11]. TNF-α injected into rat sciatic nerve stimulated neuropathic pain behaviour [12] and TNF-α mRNA levels were increased in peripheral nerve tissue from AIDS patients [13]. Furthermore, genetic association studies have linked polymorphisms and haplotypes from *TNF* and surrounding genes with increased risk of HIV-SN in Africans [14], Asians and Caucasians [15].

Chemokines produced in cutaneous tissues can bind to their receptors expressed on neuronal and inflammatory cells, initiating damage to the nerves. CCR5 and CXCR4 are co-receptors supporting HIV-1 entry [16]. CCR1, CCR2, CCR4, CCR5, CXCR4 and CX3CR1 are expressed on subpopulations of sensory neurons and their axons [17, 18]. CCR2, CCR5 and CXCR4 are upregulated in primary sensory neurons and adjacent non-neuronal cells following peripheral nerve injury in animal models [19, 20]. HIV-1 envelope glycoprotein 120 (gp120) may bind CCR5 and/or CXCR4 on nerve cells causing direct axonal damage [21], but there is no evidence of HIV infecting peripheral nerves in humans. In primary DRG cultures, gp120 mediated neuronal toxicity via TNF-α/TNF receptor (TNFR)-1 signalling [22]. CXCR4 and CCR5 ligation by CXCL12 and CCL5 (respectively) mimicked neurotoxicity induced by gp120 [22]. Administration of gp120 into rat sciatic nerve, upregulated CCL2/CCR2 and

triggered hypernociception [23]. CCR2 expression was upregulated on primary sensory neurons and Schwann cells after peripheral nerve injury [24], and CCR2-knockout mice showed reduced pain behaviour following partial ligation of sciatic nerves [25]. CX3CL1 can recruit macrophage expressing CX3CR1. CX3CR1 was upregulated on spinal microglia and DRG glial satellite cells following peripheral nerve injury [26], and CX3CR1-deficient mice showed reduced neuropathic pain behaviour [27].

There is a reasonable consensus linking HIV-SN with a reduced IENFD [28, 29], but no studies have addressed whether HIV-SN is associated with critical chemokine signalling pathways. Here we present evidence on the *ex vivo* expression of chemokine receptors on infiltrating $CD14^+$ and $CD3^+$ cells around nerves in skin biopsies from HIV+ patients exposed to modern ART regimens that excluded the known neurotoxic agents. We believe we are the first to investigate chemokine signalling pathways and IENFD in this context. These results will enhance the knowledge of the underlying pathogenesis of HIV-SN in the modern era of HIV care.

Materials and Methods

Patients and controls

HIV+ patients treated at Cipto Mangunkusumo Hospital, Jakarta, Indonesia, were screened for SN using the AIDS Clinical Trials Group Brief Peripheral Neuropathy Screen (ACTG-BPNS), a validated tool based on detection of clinical signs (reduced/absent ankle reflexes or absent/diminished vibration sense) and symptoms (pain, aching, burning, pins and needles, or numbness) of neuropathy [30]. We used the standard ACTG-BPNS case definition for HIV-SN: bilateral presence of at least one clinical sign and at least one symptom. Patients had received antiretroviral therapy for at least 12 months (median: 4.7 years [range: 1 – 12]) and had never received stavudine. Biopsies from 14 HIV+ participants (HIV-SN+ n=5, HIV-SN-n=9) were used. Control biopsies were obtained from Asian volunteers from Jakarta (male, n=1) and Curtin University, Australia (females, n=3). All donors are described in Supplementary Table 1. The study was approved by the Ethics Committee of the Faculty of Medicine, University of Indonesia (579/UN2.F1/ETIK/2014) and validated by Curtin University (HR210-2015). All participants gave written informed consent.

Sample collection and preservation

Local anaesthetic was injected and 3mm punch skin biopsies were collected ~10cm above the lateral malleolous on the distal leg, under sterile conditions. Biopsies were placed in 4% Paraformaldehyde-Lysine-Periodate fixative for 12-24 hours at 4°C before transfer to glycerol-based cryoprotectant (20% glycerol, 20% 0.4M Sorrenson's Phosphate Buffer and 60% dH$_2$O) for storage at -20°C. Biopsies were cut perpendicular to the epidermal surface on a freeze cryostat sliding microtome (Microm HM550; Thermo Scientific, Waltham, MA) set at 50µM, placed into antifreeze (33% glycerol, 33% ethylene glycol and 10% 2x phosphate buffer and dH$_2$O) and stored at -20°C for immunochemistry (IHC).

Immunochemical staining

Staining was performed in 24-well plates. Sections were bleached with 0.25% potassium permanganate (15 minutes, room temperature), washed with 1mL Tris-buffered saline (TBS) containing 0.1% Triton-X, and treated with 5% oxalic acid (2 minutes). Sections were then

blocked with Image-iT FX Signal Enhancer (Invitrogen, Carlsbad, CA) for 30 minutes. This solution was removed before the addition of primary antibodies.

To identify chemokine receptors on CD14$^+$ cells, sections were treated (overnight, 4°C) with mouse-monoclonal IgG antibodies against CCR2, CCR5, CXCR3 or CXCR4 (5μg/ml; R&D Systems, Minneapolis, MN) or CX3CR1 (10μg/ml; Biolegend, San Diego, CA), biotinylated polyclonal sheep IgG anti-CD14 (R&D systems, Minneapolis, MN) and polyclonal rabbit IgG anti-protein-gene-product 9.5 (PGP9.5; 2μg/ml) to detect nerves (Abcam, Cambridge, MA). Sections were washed five times with TBS, followed by six 1-hour washes before adding secondary antibodies; goat anti-mouse IgG FITC (20μg/ml), donkey anti-rabbit IgG Dylight (5μg/ml; Abcam) and AlexaFluor® fluorochrome streptavidin (20μg/ml; Invitrogen). Secondary antibodies were diluted in 2% donkey, goat and human serum and applied overnight at 4˚C.

To identify chemokine receptors on CD3$^+$ cells, sections were treated (overnight, 4°C) with polyclonal goat IgG against CCR2, CCR5, CXCR4 (20μg/ml) or CXCR3 (10μg/ml), mouse-polyclonal IgG anti-CD3 (10μg/ml; Novus Biologicals, Littleton, CO) and anti PGP9.5 (as above). Sections were washed as described above and treated with biotinylated donkey anti-goat IgG (20μg/ml; Abcam). Sections were blocked with 1% goat serum for 30 minutes before addition of AlexaFluor® fluorochrome streptavidin (20μg/ml; Invitrogen), goat anti-mouse IgG FITC (20μg/ml) and donkey anti-rabbit IgG (5μg/ml; Abcam). Secondary antibodies were diluted in 1% goat serum and 2% donkey serum, and applied overnight at 4°C. Stained sections were washed 6 times, incubated with 4',6-diamidino2-phylindole, diyhdrochloride (10 minutes) (Invitrogen), washed twice with TBS, mounted using Shandon Immumount (Thermo Fisher Scientific, Waltham, MA) and coverslips (#1.5, Proscitech, Queensland, Australia) before viewing. One section stained only with secondary antibodies was included in each run as a negative control.

Visualisation of sections using confocal microscopy

Images were acquired using an inverted Nikon A1+ confocal microscope with NIS-Elements confocal software (Nikon Instruments, Tokyo, Japan). Images were collected at digital scan

resolution 0.62μm/pixel, pixel dwell 4.8 with 1024 resolution using a 20x Plan Apo dry objective (N.A. 0.75). Sequential laser scanning was performed using four lasers; 405nm (450/50 filter), 488nm (525/50 filter), 561nm (595/50 filter) and 640nm (700/75 filter) to view nuclei, chemokine receptors, nerve fibres and $CD14^+$ or $CD3^+$ cells respectively. The position of the top and bottom of the image was recorded before multiple images were taken in a z-series, collected according to Nyquist criteria. Equivalent thresholds were applied across images to visualise nerves (white), chemokine receptors (red) and $CD14^+$ or $CD3^+$ (green). Chemokine receptors co-located with either $CD14^+$ or $CD3^+$ cells appeared yellow.

Intraepidermal nerve fibre density (IENFD)

NIS-Elements Advanced Research software (Nikon Instruments, Tokyo, Japan) was used to acquire three $0.5mm^2$ sections per biopsy (only 2 samples were available for one participant). Sections were coded and nerve fibres were counted by six investigators using standardised rules for IENFD quantification [31]. In brief, single IENF crossing the dermal-epidermal junction are counted with secondary branching excluded from quantification. The average count across the three sections per biopsy was multiplied by 2 to generate IENFD per mm^2 area of skin for each participant (Supplementary Figure 1).

We computed Light's κ for exact agreement (0 tolerance) between the six raters, treating rating as a weighted variable and using squared distance. A bootstrap 95% confidence interval (n = 1000 resamples) was calculated using the bias-corrected and accelerated bootstrap method. The analysis yielded a Light's κ = 0.79 (95%CI: 0.61 to 0.91); the point estimate indicating strong inter-rater agreement, with the confidence interval indicating moderate to strong agreement [32].

Results

Intraepidermal nerve fibre density was generally reduced in HIV-SN+ patients

HIV-SN+ (*n*=5) and HIV-SN- (*n*=9) patients were matched for age, height, time on ART and CD4$^+$ T cell counts (Supplementary Table 1). Healthy controls (HC, *n*=4) were also matched with the patients by age and height. All donors were of South East Asian ancestry. **Figure 1** shows confocal images from two HC (panels A and B), two HIV-SN- patients (panels C and D) and two HIV-SN+ patients (panels E and F) selected to represent the range seen in each group. Median (range) IENFD per square mm field were 11.2 (5.8 – 15.2), 5.8 (1.3 – 14.0) and 3.0 (0.8 – 9.7) in HC, HIV-SN- and HIV-SN+ groups, respectively. The IENFD tended to be reduced in HIV-SN+ patients compared with HC, but the study was not powered to find a significant difference (Supplementary Tables 1, 2, Supplementary Figure 1). A reduction in the length of nerve fibres within the epidermis of HIV-SN+ patients was common. CD14$^+$ macrophages were visible in sections from HIV+ patients. Many were adjacent to blood vessels, scattered within cutaneous tissue or adjacent nerve fibres.

CX3CR1 was expressed on CD14$^+$ cells adjacent to peripheral nerves in HIV-SN+ patients

Sections were stained to visualise expression of CX3CR1 on infiltrating CD14$^+$ cells (**Figure 1**). CX3CR1 expression was extremely rare in the three sections from HC (panels A and B). They were also rare in sections from three HIV-SN- patients (e.g. panels C and D). Few CX3CR1$^+$ cells were seen in two of three sections from HIV-SN+ patients (panels E and F). In all sections from HIV-SN+ patients, CX3CR1 was co-located with CD14 (yellow arrows) and was closely associated with the subepidermal nerve plexi (**Figure 1,** panels E and F). This is consistent with a role for the receptor in HIV-SN.

CCR2 is upregulated in HIV-SN+ skin and predominantly expressed by CD3$^+$ cells

Sections were stained to visualise CCR2 on infiltrating CD14$^+$ or CD3$^+$ cells (**Figure 2**). Very few CCR2$^+$ cells were evident in HC (e.g. panels A and B). Two of eight stained sections from HIV-SN- cases displayed detectable CCR2$^+$ cells (e.g. panel D), whereas all seven sections

from five HIV-SN+ cases displayed CCR2 expression (e.g. panels E and F). The HIV-SN- patient expressing CCR2 most clearly (patient 11; not shown) had the lowest IENFD and a case review uncovered a history of Stevens Johnson Syndrome – an inflammation of the skin. The patient was excluded from further IHC. Most CCR2 was co-located with CD3 (panels D and F, yellow arrows). CD14$^+$ cells were visible but rarely expressed CCR2 (panels A, C, E).

CCR5 is upregulated and associated with peripheral nerves in HIV-SN+ skin sections

Sections were also stained to visualise expression of CCR5 on infiltrating CD14$^+$ or CD3$^+$ cells (**Figure 3**). CCR5$^+$ cells were very rare in HC (panels A and B). Isolated positive cells were seen in two of five samples from HIV-SN- (panels C and D) and five of five samples from HIV-SN+ patients, with some cells located close to nerve fibres (panels E and F). CCR5 was co-located with CD3 (yellow arrows, panels D and F), but not CD14 (panels A, C and E).

CXCR3 was expressed by scattered CD3$^+$ cells in all HIV+ patients

CXCR3$^+$ cells were visible in blood vessels present in some sections from all groups. CXCR3$^+$ cells located closely with CD14$^+$ cells but the two markers did not co-stain (**Figure 4**: panels A, C, E). In addition, variable numbers of CD3$^+$ CXCR3$^+$ cells were seen scattered in the tissues, so that some were adjacent to nerves in all eight sections from HIV-SN- and three sections from HIV-SN+ patients. Fewer positive cells were seen in samples from HC, so expression of this marker may be a consequence of HIV infection.

CXCR4$^+$ CD3$^+$ cells were seen along the epidermis and the dermis in HIV+ patients

CXCR4$^+$ cells were seen in some but not all sections from HC (**Figure 5**. panels A and B). CXCR4 was expressed in all six sections from HIV-SN- patients (panels C and D) and three HIV-SN+ patients (panels E and F) and was distributed along the epidermis (panel C and F) or adjacent to blood vessels (panel E). Some larger cells expressed CXCR4 without CD14$^+$ (panel E). CXCR4 was expressed on a subset of CD3$^+$ cells in the dermis (panels D and F). This may reflect HIV disease rather than HIV-SN.

Discussion

We have developed a protocol that identifies cells and receptors that could contribute to the damage of small nerve fibres and form the basis of HIV-SN. The compilation of images into z-series allowed us to follow individual nerves as if they were distributed in the tissue in just two dimensions. Counts made by multiple observers blinded to the disease phenotype provide reliable quantification of IENFD (Supplementary Figure 1). The median IENFD at the distal leg of normal controls was 11.2 per mm^2. This is consistent with an earlier study with the reference range of 13.8$\pm$6.7 per mm^2 [33]. IENFD was generally reduced in HIV-SN+ patients and variable in those without HIV-SN. The wide range of nerve fibre densities in HIV-SN- patients may reflect early lesions not detected by the ACTG-BPNS. A recent longitudinal study of 150 Thai HIV+ individuals found IENFD measurements did not distinguish individuals with HIV-SN or signal the onset of neuropathic signs/symptoms [34]. However, IENFD decreases with increasing age [35]. Here all donors were 25 to 47 years old so any effect from age is likely to be minimal. We were also unable to assess associations with genotype [14, 36], but all participants were of South East Asian descent.

In addition to a reduction in the number of nerves in the epidermis, our methods demonstrate a reduction in cutaneous nerve fibre length in adults with HIV-SN (Figure 1, panels E) and in some HIV-SN- cases (Figure 1, panel C). It is unlikely that the loss of nerves reflects direct infection by HIV [9]. However, HIV-infected macrophages may have a primary role in nerve damage or may accumulate in response to debris from destroyed axons [37]. Our results show CD14$^+$ macrophages were visible in all sections. These CD14$^+$ macrophages may release pro-inflammatory cytokines causing axonal and DRG neuronal injury [38, 39]. A recent study has linked the loss of IENFD and increased recruitment of macrophages to DRG in Simian Immunodeficiency Virus-infected macaques [40]. We show macrophages adjacent to blood vessels, scattered within cutaneous tissues and adjacent to nerve fibres. This distribution is consistent with their extravasation and migration towards the nerves, a pattern observed in other chronic inflammatory neuropathies [41]. However, these CD14$^+$ macrophages did not express CCR2, CCR5, CXCR3 or CXCR4 but did express CX3CR1.

CX3CR1[+] monocyte/macrophage are expressed in low levels and are recruited in healing tissues [42]. CX3CL1/CX3CR1 signalling is implicated in the development of neuropathic pain in animal models [27, 43-45]. Our results show CX3CR1 was minimally expressed, but CX3CR1^{+} CD14^{+} macrophages were seen near the residual nerves in sections from HIV-SN+ patients. This supports a study showing increased expression of CX3CR1 by macrophages in the sciatic nerve proximal to a site of mechanical injury and in the corresponding DRG [26]. Furthermore in a spinal nerve ligation model, CX3CR1 expression was upregulated in spinal microglia, whilst membrane-bound levels of CX3CL1 were reduced [43]. The cleavage of CX3CL1 after nerve injury may initiate activation of the low affinity purinergic P2X7 receptor, leading to the release of the lysosomal cysteine protease cathepsin S from microglia. This may mediate neural–glial interaction and neuropathic pain behavior [46]. Accordingly, the gene encoding the P2X7 receptor, P2X7R, lies in a region of linkage disequilibrium with upstream genes P2X4R and CAMKK2 and single nucleotide polymorphisms and haplotypes within this block of genes were associated with HIV-SN in South Africans HIV+ individuals [47]. Other studies suggest downstream mechanisms of CX3CR1 via p38 mitogen-activated protein kinases [43] or extracellular signal-regulated protein kinase 5 [48] may activate microglia after nerve injury. Blockade or knockout of CX3CR1 impaired neuropathic pain behaviours and reduced hypersensitivity to thermal stimuli following peripheral nerve injury in animal models [27, 43, 44]. These considerations support our evidence that CX3CR1 could have a role in HIV-SN.

Our results show CCR2, CCR5, CXCR3 and CXCR4 were co-localised with CD3 but not CD14. T-lymphocytes were observed in nerves obtained from patients with inflammatory neuropathies [49]. An immunocytochemical study investigating mononuclear cells in sural nerve biopsies from 42 HIV- and HIV+ patients with various types of peripheral neuropathy found that 72% of infiltrating mononuclear cells were CD3^{+} [50]. T-cell infiltration into the spinal dorsal horn after nerve injury was also implicated in the development of pain-like hypersensitivity in rats [51]. CCR2 is critical in recruiting T-cells in responses to axonal injury of the central nervous system [52]. CCL2/CCR2 expression were upregulated by primary sensory neurons and Schwann cells after a sciatic nerve constriction injury [24]. CCL2/CCR2 was also upregulated by gp120 injected into rat sciatic nerve. This paralleled the

development of mechanical hypernociception [23]. Accordingly, we found CCR2 was upregulated and expressed in five of five HIV-SN+ skin sections.

CCR5 and CXCR4 are co-receptors for HIV. CXCR4 was expressed in all HIV+ skin sections whilst CCR5 was more evident in skin sections from patients with SN, with some positive cells located near nerve fibres. In a study of chemokine receptors in HIV/gp120-induced neurotoxicity based on mixed neuronal/glial cerebrocortical cultures, gp120 utilized CCR5, CXCR4 or both to cause neurotoxicity [53]. Interestingly, CCL4 and CCL5 (ligands of CCR5) can inhibit gp120-induced neuronal death, whilst CXCL12 (the ligand of CXCR4) could alone, be neurotoxic. Moreover, CCR5 ligands could inhibit CXCR4/CXCL12-induced neurotoxicity [53]. Hence our finding linking CCR5 with HIV-SN may place the receptor in a complex cascade. For example; the binding of gp120 to CXCR4 on Schwann cells can cause the release of CCL5. CCL5 can stimulate the production of TNF–α by neuronal cells in DRG, leading to TNFR1-mediated neurotoxicity [22].

CXCR3 co-localized with CD3 in all HIV+ patients. CXCR3 plays role in the adaptive immune response to inflammation and viral infection [54]. Some CXCR3^{+} cells were located near damaged nerves. In patients with diabetic neuropathy, quantitative polymerase chain reaction and flow cytometric analyses showed that CXCR3^{+} CD8^{+} T-cells were recruited and infiltrated into affected tissues [55]. CXCR3 ligands, CXCL9, CXCL10 and CXCL11, released from Schwann cells can further recruit CXCR3^{+} CD8^{+} T-cell into sites of peripheral neuropathy [56]. Furthermore, Schwann cells can stimulate CD8^{+} T-cells to release TNF–α and Programmed death-ligand 1 (PD-1) leading to neuronal apoptosis [55]. In foetal neuronal cultures, ligation of CXCR3 and CXCL10 can increase intracellular calcium, which in turn increases membrane permeability and cytochrome c release. This activates caspase-9 which activates caspase-3, ultimately leading to neuronal apoptosis [56]. Caspase 3-dependent neuronal apoptosis cascades have been demonstrated in studies of gp120-induced neurotoxicity [22, 57].

Our study has some limitations. First, tissue samples were small, and sampling error remains a possible issue as we did not scan the entire biopsy. Second, we used one validated but simple clinical tool to distinguish patients with structural changes to the cutaneous nerves (HIV-SN+) from those without (HIV-SN-). We cannot exclude the possibility that some of our "SN free" HIV+ patients may have had early, sub-clinical peripheral nerve lesions that were not detected by this tool. Third, the presence of chemokine receptors in skin tissues does not prove that their signalling is critical. However, we have linked CD14^{+} macrophages expressing CX3CR1, and CD3^{+} T-cells expressing CCR2 and/or CCR5 with HIV-SN in skin sections from HIV+ individuals. The cells may have a role in the loss of nerves (evident from the IENFD) or may impact upon nerve function creating the characteristic signs and symptoms of HIV-SN (numbness, tingling, pain, reduced vibration sense, etc.). Expression of CXCR3 and CXCR4 was linked with HIV disease as these receptors were found in all sections from patients. Further investigation is needed with longitudinal studies including samples collected during earlier phases of HIV-SN.

References

1. Hall CD, Snyder CR, Messenheimer JA, Wilkins JW, Robertson WT, Whaley RA, et al. **Peripheral neuropathy in a cohort of human immunodeficiency virus—infected patients: incidence and relationship to other nervous system dysfunction**. *Archives of neurology* 1991; **48**:1273-1274.

2. McArthur JH. **The reliability and validity of the subjective peripheral neuropathy screen**. *Journal of the Association of Nurses in AIDS Care* 1998; **9**:84-94.

3. Cherry CL, Affandi JS, Imran D, Yunihastuti E, Smyth K, Vanar S, et al. **Age and height predict neuropathy risk in patients with HIV prescribed stavudine**. *Neurology* 2009; **73**:315.

4. Wadley AL, Cherry CL, Price P, Kamerman PR. **HIV Neuropathy Risk Factors and Symptom Characterization in Stavudine- Exposed South Africans**. *Journal of Pain and Symptom Management* 2011; **41**:700-706.

5. Ellis RJ, Rosario D, Clifford DB, McArthur JC, Simpson D, Alexander T, et al. **Continued High Prevalence and Adverse Clinical Impact of Human Immunodeficiency Virus–Associated Sensory Neuropathy in the Era of Combination Antiretroviral Therapy: The CHARTER Study**. *Archives of Neurology* 2010; **67**:552-558.

6. Cherry C, Kamerman P, Bennett DLH, Rice ASC. **HIV-associated sensory neuropathy: still a problem in the post-stavudine era?** *Future Virology* 2012; **7**:849-854.

7. Arenas-Pinto A, Thompson J, Musoro G, Musana H, Lugemwa A, Kambugu A, et al. **Peripheral neuropathy in HIV patients in sub-Saharan Africa failing first-line therapy and the response to second-line ART in the EARNEST trial**. *Journal of Neurovirology* 2016; **22**:104-113.

8. Polydefkis M, Yiannoutsos CT, Cohen BA, Hollander H, Schifitto G, Clifford DB, et al. **Reduced intraepidermal nerve fiber density in HIV-associated sensory neuropathy**. *Neurology* 2002; **58**:115-119.

9. De La Monte SM, Gabuzda DH, Ho DD, Brown RH, Hedley-Whyte ET, Schooley RT, et al. **Peripheral neuropathy in the acquired immunodeficiency syndrome**. *Annals of Neurology* 1988; **23**:485-492.

10. Herzberg U, Sagen J. **Peripheral nerve exposure to HIV viral envelope protein gp120 induces neuropathic pain and spinal gliosis**. *Journal of Neuroimmunology* 2001; **116**:29-39.

11. Keswani CS, Pardo AC, Cherry LC, Hoke CA, McArthur CJ. **HIV- associated sensory neuropathies**. *AIDS* 2002; **16**:2105-2117.

12. Wagner R, Myers RR. **Endoneurial injection of TNF-[alpha] produces neuropathic pain behaviors**. *Neuroreport* 1996; **7**:2897-2902.

13. Tyor WR, Wesselingh SL, Griffin JW, McArthur JC, Griffin DE. **Unifying hypothesis for the pathogenesis of HIV-associated dementia complex, vacuolar myelopathy, and sensory neuropathy**. *Journal of AIDS* 1995; **9**:379-388.

14. Wadley AL, Kamerman PR, Chew CSN, Lombard Z, Cherry CL, Price P. **A polymorphism in IL4 may associate with sensory neuropathy in African HIV patients**. *Molecular immunology* 2013; **55**:197.

15. Chew C, Cherry C, Imran D, Yunihastuti E, Kamarulzaman A, Varna S, et al. **Tumour necrosis factor haplotypes associated with sensory neuropathy in Asian and Caucasian human immunodeficiency virus patients**. *Tissue Antigens* 2011; **77**:126.

16. Bleul CC, Wu L, Hoxie JA, Springer TA, Mackay CR. **The HIV coreceptors CXCR4 and CCR5 are differentially expressed and regulated on human T lymphocytes**. *Proceedings of the National Academy of Sciences* 1997; **94**:1925-1930.

17. Oh SB, Tran PB, Gillard SE, Hurley RW, Hammond DL, Miller RJ. **Chemokines and glycoprotein120 produce pain hypersensitivity by directly exciting primary nociceptive neurons**. *The Journal of Neuroscience* 2001; **21**:5027.

18. Abbadie C. **Chemokines, chemokine receptors and pain**. *Trends in Immunology* 2005; **26**:529-534.

19. White FA, Sun J, Waters SM, Ma C, Ren D, Ripsch M, et al. **Excitatory monocyte chemoattractant protein-1 signaling is up-regulated in sensory neurons after chronic compression of the dorsal root ganglion**. *Proceedings of the National Academy of Sciences USA* 2005; **102**:14092-14097.

20. Bhangoo S, Ren D, Miller RJ, Henry KJ, Lineswala J, Hamdouchi C, et al. **Delayed Functional Expression of Neuronal Chemokine Receptors Following Focal Nerve Demyelination in the Rat: A Mechanism for the Development of Chronic Sensitization of Peripheral Nociceptors**. *Molecular Pain* 2007; **3**.

21. Melli G, Keswani SC, Fischer A, Chen W, Höke A. **Spatially distinct and functionally independent mechanisms of axonal degeneration in a model of HIV-associated sensory neuropathy**. *Brain* 2006; **129**:1330-1338.

22. Keswani SC, Polley M, Pardo CA, Griffin JW, McArthur JC, Hoke A. **Schwann cell chemokine receptors mediate HIV- 1 gp120 toxicity to sensory neurons**. *Annals of Neurology* 2003; **54**:287-296.

23. Bhangoo SK, Ripsch MS, Buchanan DJ, Miller RJ, White FA. **Increased chemokine signaling in a model of HIV1- associated peripheral neuropathy**. *Molecular Pain* 2009; **5**:48-48.

24. Zhang J, Koninck Y. **Spatial and temporal relationship between monocyte chemoattractant protein-1 expression and spinal glial activation following peripheral nerve injury**. *Journal of Neurochemistry* 2006; **97**:772-783.

25. Abbadie C, Lindia JA, Cumiskey AM, Peterson LB, Mudgett JS, Bayne EK, et al. **Impaired Neuropathic Pain Responses in Mice Lacking the Chemokine Receptor CCR2**. *Proceedings of the National Academy of Sciences USA* 2003; **100**:7947-7952.

26. Holmes FE, Arnott N, Vanderplank P, Kerr NCH, Longbrake EE, Popovich PG, et al. **Intra-neural administration of fractalkine attenuates neuropathic pain-related behaviour**. *Journal of Neurochemistry* 2008; **106**:640-649.

27. Staniland AA, Clark AK, Wodarski R, Sasso O, Maione F, D'acquisto F, et al. **Reduced inflammatory and neuropathic pain and decreased spinal microglial response in fractalkine receptor (CX3CR1) knockout mice**. *Journal of Neurochemistry* 2010; **114**:1143-1157.

28. Kokotis P, Schmelz M, Papadimas GK, Skopelitis EE, Aroni K, Kordossis T, et al. **Polyneuropathy induced by HIV disease and antiretroviral therapy**. *Clinical Neurophysiology* 2013; **124**:176-182.

29. Zhou L, Kitch DW, Evans SR, Hauer P, Raman S, Ebenezer GJ, et al. **Correlates of epidermal nerve fiber densities in HIV-associated distal sensory polyneuropathy**. *Neurology* 2007; **68**:2113.

30. Cherry CL, Wesselingh SL, Lal L, McArthur JC. **Evaluation of a clinical screening tool for HIV- associated sensory neuropathies**. *Neurology* 2005; **65**:1778.

31. Lauria G, Hsieh ST, Johansson O, Kennedy WR, Leger JM, Mellgren SI, et al. **European Federation of Neurological Societies/Peripheral Nerve Society Guideline on the use of skin**

biopsy in the diagnosis of small fiber neuropathy. *European Journal of Neurology* 2010; **17**:903-e949.

32. McHugh ML. **Interrater reliability: the kappa statistic**. *Biochemia Medica* 2012; **22**:276-282.

33. McArthur JC, Stocks EA, Hauer P, Cornblath DR, Griffin JW. **Epidermal nerve fiber density: Normative reference range and diagnostic efficiency**. *Archives of Neurology* 1998; **55**:1513-1520.

34. Shikuma CM, Bennett K, Ananworanich J, Gerschenson M, Teeratakulpisarn N, Jadwattanakul T, et al. **Distal leg epidermal nerve fiber density as a surrogate marker of HIV-associated sensory neuropathy risk: risk factors and change following initial antiretroviral therapy**. *Journal of Neurovirology* 2015; **21**:525.

35. Provitera V, Gibbons CH, Wendelschafer-Crabb G, Donadio V, Vitale DF, Stancanelli A, et al. **A multi-center, multinational age- and gender-adjusted normative dataset for immunofluorescent intraepidermal nerve fiber density at the distal leg**. *European Journal of Neurology* 2016; **23**:333-338.

36. Hulgan TT, Levinson ER, Gerschenson CM, Phanuphak JN, Ananworanich MJ, Teeratakulpisarm CN, et al. **Epidermal nerve fiber density, oxidative stress, and mitochondrial haplogroups in HIV-infected Thais initiating therapy**. *AIDS* 2014; **28**:1625-1633.

37. Laast VA, Shim B, Johanek LM, Dorsey JL, Hauer PE, Tarwater PM, et al. **Macrophage-Mediated Dorsal Root Ganglion Damage Precedes Altered Nerve Conduction in SIV-Infected Macaques**. *American Journal of Pathology* 2011; **179**:2337-2345.

38. Purwata T. **High TNF-alpha plasma levels and macrophages iNOS and TNF-alpha expression as risk factors for painful diabetic neuropathy**. *Journal of Pain Research* 2011; 2011:169-175.

39. Uçeyler N, Rogausch JP, Toyka KV, Sommer C. **Differential expression of cytokines in painful and painless neuropathies**. *Neurology* 2007; **69**:42.

40. Lakritz JR, Bodair A, Shah N, Amp, Apos, Donnell R, et al. **Monocyte Traffic, Dorsal Root Ganglion Histopathology, and Loss of Intraepidermal Nerve Fiber Density in SIV Peripheral Neuropathy**. *American Journal of Pathology* 2015; **185**:1912-1923.

41. Griffin JW, Stoll G, Li CY, Tyor W, Cornblath DR. **Macrophage responses in inflammatory demyelinating neuropathies**. *Annals of Neurology* 1990; 27 Suppl:S64.

42. Awojoodu AO, Ogle ME, Sefcik LS, Bowers DT, Martin K, Brayman KL, et al. **Sphingosine 1-phosphate receptor 3 regulates recruitment of anti-inflammatory monocytes to microvessels during implant arteriogenesis**. *Proceedings of the National Academy of Sciences USA* 2013; **110**:13785.

43. Zhuang Z-Y, Kawasaki Y, Tan P-H, Wen Y-R, Huang J, Ji R-R. **Role of the CX3CR1/p38 MAPK pathway in spinal microglia for the development of neuropathic pain following nerve injury-induced cleavage of fractalkine**. *Brain Behavior and Immunity* 2007; **21**:642-651.

44. Bian C, Zhao Z-Q, Zhang Y-Q, Lü N, Shamji M. **Involvement of CX3CL1/CX3CR1 Signaling in Spinal Long Term Potentiation**. *PLoS ONE* 2015; **10**.

45. Kiguchi N, Kobayashi Y, Kishioka S. **Chemokines and cytokines in neuroinflammation leading to neuropathic pain**. *Current Opinion in Pharmacology* 2011; **12**:55-61.

46. Clark AK, Wodarski R, Guida F, Sasso O, Malcangio M. **Cathepsin S release from primary cultured microglia is regulated by the P2X7 receptor**. *Glia* 2010; **58**:1710-1726.

47. Goullee H, Wadley A, Cherry C, Allcock R, Black M, Kamerman P, et al. **Polymorphisms in CAMKK2 may predict sensory neuropathy in African HIV patients**. *Journal of NeuroVirology* 2016; **22**:508-517.

48. Sun JL, Xiao C, Lu B, Zhang J, Yuan XZ, Chen W, et al. **CX3CL1/CX3CR1 regulates nerve injury-induced pain hypersensitivity through the ERK5 signaling pathway**. *Journal of Neuroscience Research* 2013; **91**:545-553.

49. Winer J, Hughes S, Cooper J, Ben-Smith A, Savage C. **gamma delta T cells infiltrating sensory nerve biopsies from patients with inflammatory neuropathy**. *Journal of Neurology* 2002; **249**:616.

50. Cornblath DR, Griffin DE, Welch D, Griffin JW, McArthur JC. **Quantitative analysis of endoneurial T-cells in human sural nerve biopsies**. *Journal of Neuroimmunology* 1990; **26**:113-118.

51. Costigan M, Moss A, Latremoliere A, Johnston C, Verma-Gandhu M, Herbert TA, et al. **T-cell infiltration and signaling in the adult dorsal spinal cord is a major contributor to neuropathic pain-like hypersensitivity**. *Journal of Neuroscience* 2009; **29**:14415-14422.

52. Babcock A, Kuziel W, Rivest S, Owens T. **Chemokine Expression by Glial Cells Directs Leukocytes to Sites of Axonal Injury in the CNS**. *Journal of Neuroscience* 2003; **23**:7922-7930.

53. Kaul M, Ma Q, Medders KE, Desai MK, Lipton SA. **HIV-1 coreceptors CCR5 and CXCR4 both mediate neuronal cell death but CCR5 paradoxically can also contribute to protection**. *Cell Death and Differentiation* 2006; **14**:296.

54. Kohlmeier JE, Reiley WW, Perona-Wright G, Freeman ML, Yager EJ, Connor LM, et al. **Inflammatory chemokine receptors regulate CD8+ T cell contraction and memory generation following infection**. *Journal of Experimental Medicine* 2011; **208**:1621-1634.

55. Tang W, Lv Q, Chen XF, Zou JJ, Liu Zm, Shi YQ. **CD8+ T Cell-Mediated Cytotoxicity toward Schwann Cells Promotes Diabetic Peripheral Neuropathy**. *Cellular Physiology and Biochemistry* 2013; **32**:827-837.

56. Sui Y, Stehno-bittel L, Li S, Loganathan R, Dhillon NK, Pinson D, et al. **CXCL10- induced cell death in neurons: role of calcium dysregulation**. *European Journal of Neuroscience* 2006; **23**:957-964.

57. Garden GA, Budd SL, Tsai E, Hanson L, Kaul M, D'Emilia DM, et al. **Caspase cascades in human immunodeficiency virus-associated neurodegeneration**. *Journal of Neuroscience* 2002; **22**:4015.

Figure 1. Representative confocal images showing expression of CX3CR1 and CD14 in skin from two HC (A, B), HIV-SN- (C, D) and HIV-SN+ (E, F) patients. Abundant thin intraepidermal nerve fibres run from the dermis innervating the basement membrane and epidermis in HC skin section. The median nerve count (IEFND) was 11.2 [range: 5.8 – 15.2] fibres per mm^2 skin area. IENFD was variable in HIV-SN- sections (5.8 [1.3 – 14.0]) and slightly lower in HIV-SN+ (3.0 [0.8 – 9.7]). CX3CR1 was rare in HC skin sections and minimally expressed skin sections from patients. However, CX3CR1 expression was closely associated with epidermal nerves in HIV-SN+ sections, and co-localised with CD14$^+$ cells (E, F; yellow arrows). The white line represents 100μm.

Figure 2. **Representative confocal images showing expression of CCR2 with CD14 (left) or CD3 (right) in skin from HC (A, B), HIV-SN- (C, D) and HIV-SN+ (E, F) patients.** CCR2 expression was rare in HC. Two of eight stained sections from HIV-SN- patients had detectable CCR2$^+$ cells, whereas seven of seven sections from five HIV-SN+ cases displayed CCR2. Some CCR2$^+$ cells were located close to nerves. CCR2 was rarely expressed on CD14$^+$ cells (E), but was seen on CD3$^+$ cells (D, F; yellow arrows).

Figure 3. Representative confocal images showing expression of CCR5 with CD14 (left) or CD3 (right) in skin from HC (A, B), HIV-SN- (C, D) and HIV-SN+ (E, F) patients. CCR5$^+$ cells were rare in sections from HC (A, B), but expression was up-regulated in sections from HIV+ patients; HIV-SN- (two of five) and HIV-SN+ (six of six). CCR5 was predominantly co-localised with CD3 (D, F; yellow arrows). Some CCR5$^+$ cells were located close to nerve fibres in sections from HIV-SN+ patients (E, F).

Figure 4. **Representative confocal images showing expression of CXCR3 with CD14 (left) or CD3 (right) in skin from HC (A, B), HIV-SN- (C, D) and HIV-SN+ (E, F) patients.** CXCR3 was rare in HC, mostly surrounding dermal blood vessels. CXCR3 was highly expressed in sections from all HIV+ patients, and most commonly co-located with CD3 (D, F; yellow arrows). An expanded red box (E) highlights the close proximity of CD14$^+$ (green) and CXCR3$^+$ (red) cells on the nerve. A yellow box (F) shows the co-localisation of CD3 and CXCR3 (yellow) adhering to a cutaneous nerve in a HIV-SN+ section.

Figure 5. Representative confocal images showing expression of CXCR4 with CD14 (left) or CD3 (right) in skin from HC (A, B), HIV-SN- (C, D) and HIV-SN+ (E, F) patients. CXCR4 was upregulated in the epidermis and the dermis of HIV+ patients, with mixed patterns of expression (C, D, E, F). CXCR4 was rarely expressed on CD14$^+$ cells (A, C, E) but was seen on CD3$^+$ cells (D, F; yellow arrows).
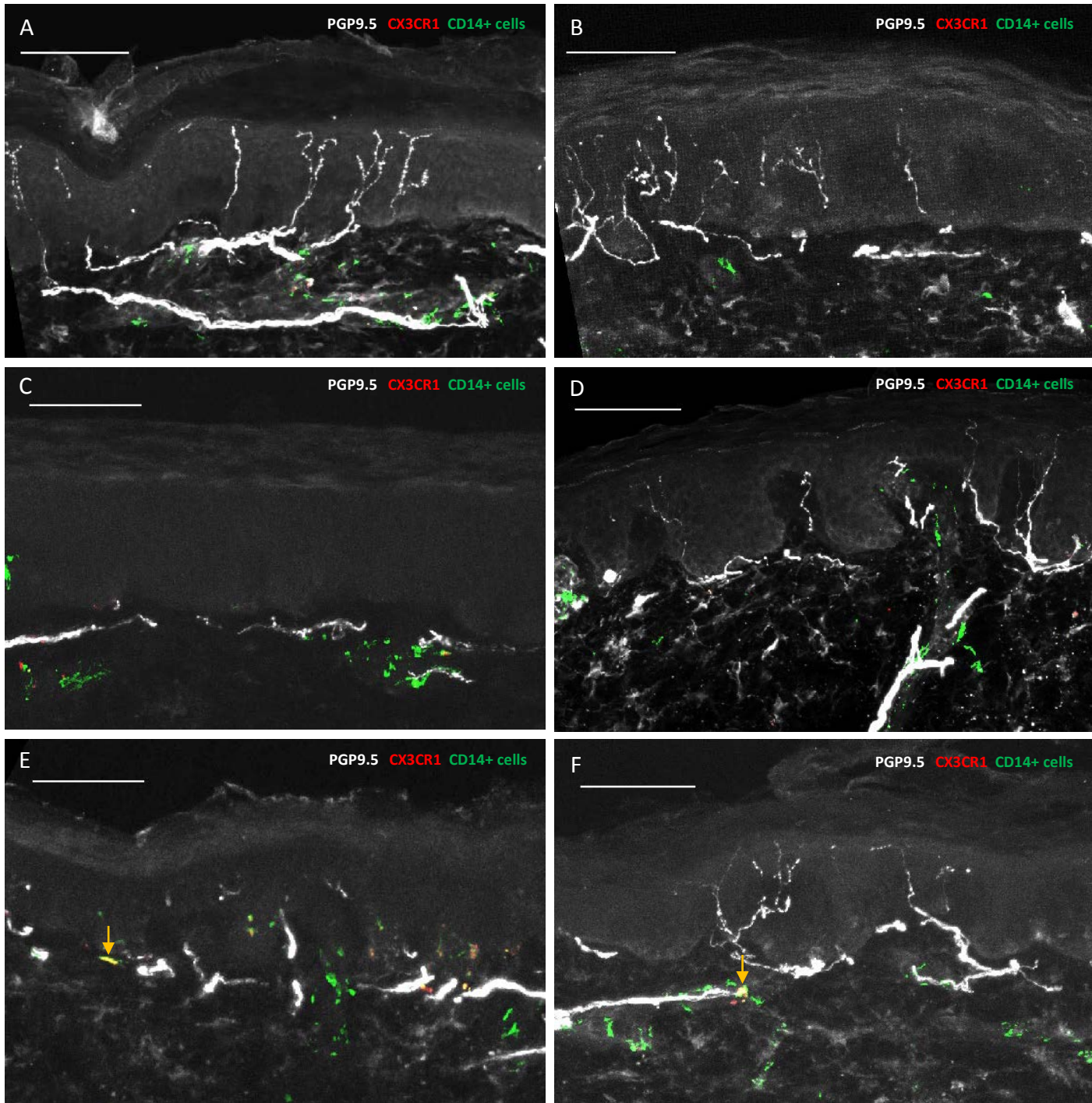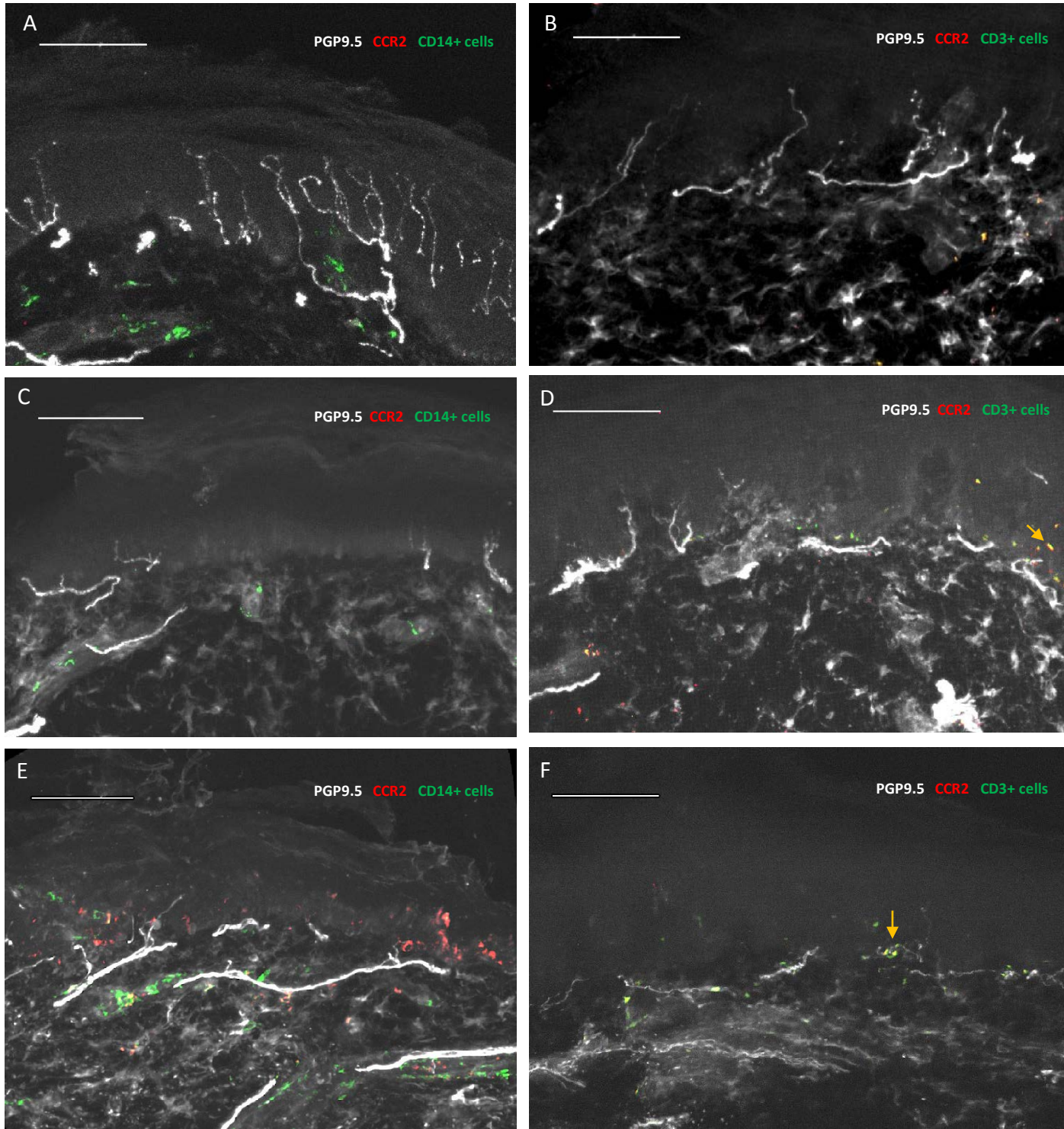
CX3CR1

Figure 1

CCR2
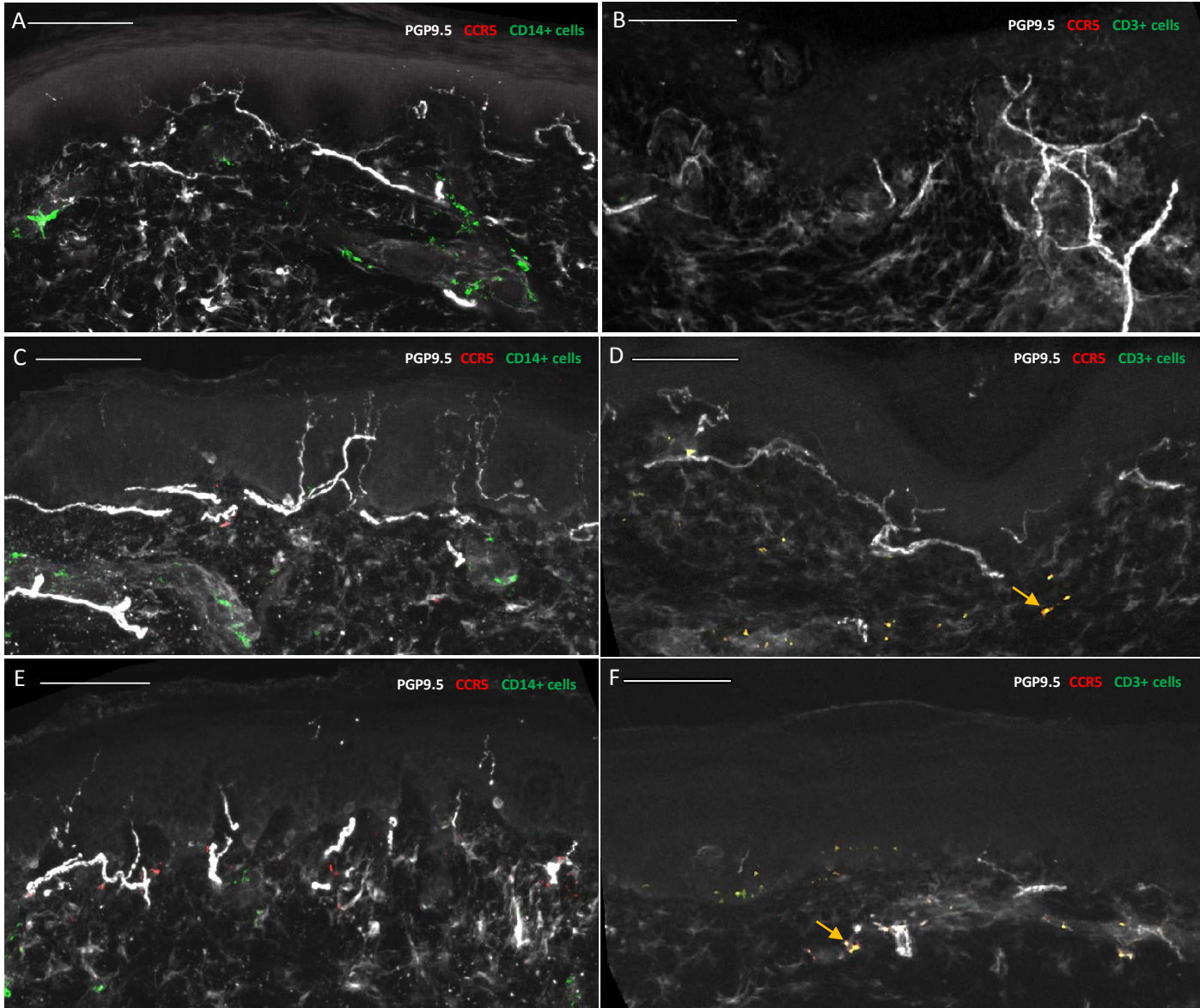

Figure 2

CCR5

Figure 3
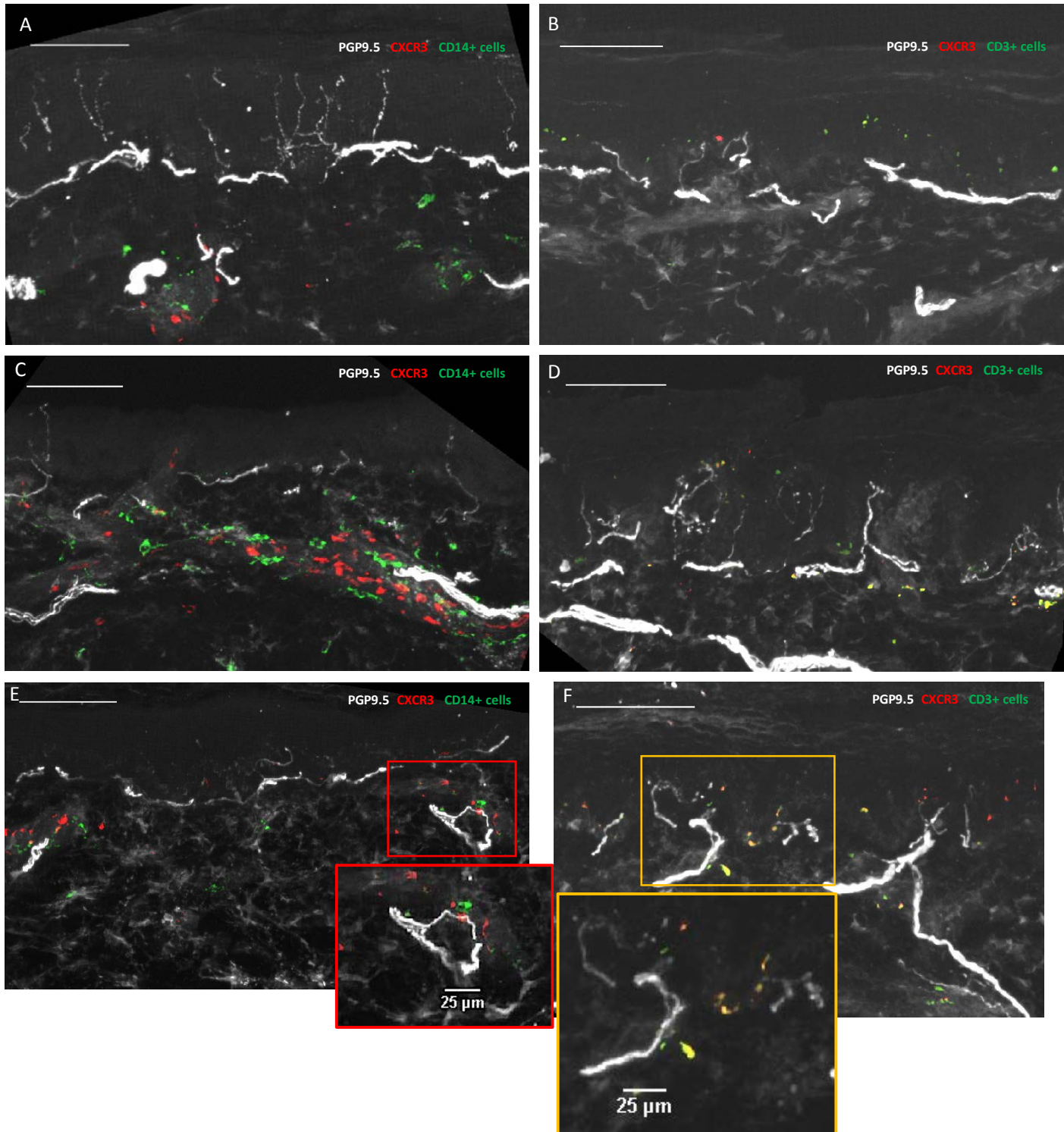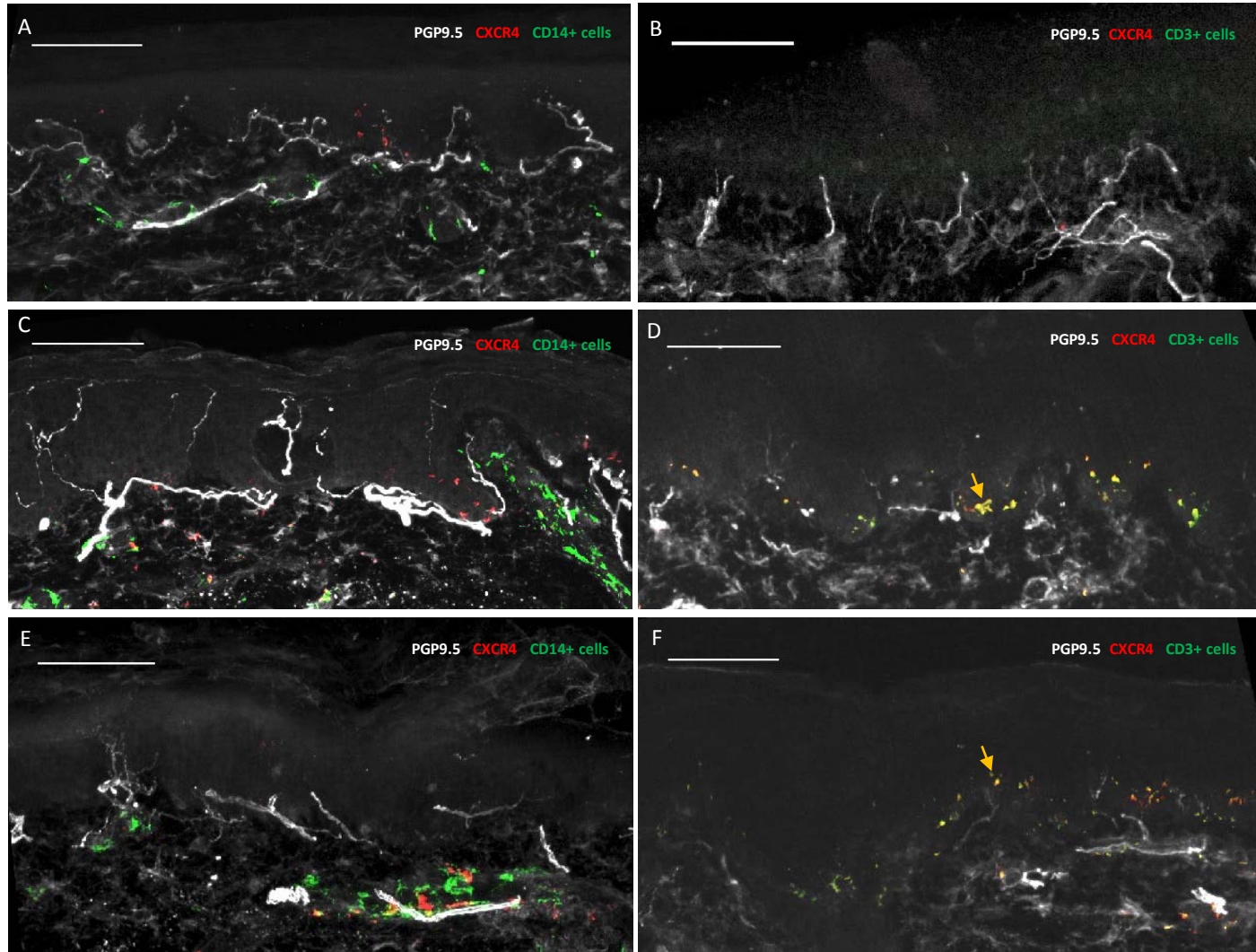
CXCR3

Figure 4

CXCR4

Figure 5

SUPPLEMENTS

Table 1; Characteristics of patients and healthy controls (HC)

Donor	BPNST[a]	Gender	Age (years)	Height (cm)	Time on ART (years)	Last CD4 count (cell/uL)	IEFND[b] (per mm^2)
Patient 1	HIV-SN+	Female	33	158	7	406	1.6
Patient 2	HIV-SN+	Female	33	167	7.5	729	9.7
Patient 3	HIV-SN+	Male	34	175	5	714	3.0
Patient 4	HIV-SN+	Male	47	167	6.8	284	4.6
Patient 5	HIV-SN+	Male	45	167	3.5	300	0.8
Patient 6	HIV-SN-	Male	38	179	8.7	626	6.7
Patient 7	HIV-SN-	Female	41	150	1	435	6.6
Patient 8	HIV-SN-	Male	35	165	12	693	5.4
Patient 9	HIV-SN-	Female	32	165	3.6	385	9.0
Patient 10	HIV-SN-	Male	44	171	2.8	84	4.0
Patient 11	HIV-SN-	Male	36	168	1	566	1.3
Patient 12	HIV-SN-	Male	25	165	1.6	653	14.0
Patient 13	HIV-SN-	Male	34	166	2.2	386	5.2
Patient 14	HIV-SN-	Female	41	150	1	448	5.8
HC1	-	Female	28	158	-	-	-
HC2	-	Female	33	162	-	-	11.2
HC3	-	Female	33	151	-	-	15.2
HC4	-	Male	37	169	-	-	5.8

[a] Brief Peripheral Neuropathy Screening Tool

[b] Inter Epithelial Nerve Fibre Density

Table 2; Summary of donor characteristics

(BPNST)	N value	Male (*n*)	Age (years)	Height (cm)	Time on ART (years)	Last CD4 (cell/uL)	IEFND (per mm²)
HIV-SN+	5	3	34 (33-47)	167 (158-175)	6.8 (3.5-7.5)	406 (284-729)	3.0 (0.8 – 9.7)
HIV-SN-	9	6	36 (25-44)	165 (150-179)	2.2 (1.0-12)	448 (84-693)	5.8 (1.3 – 14.0)
HC	4	1	33 (28-37)	160 (151-169)	n/a	n/a	11.2 (5.8 – 15.2)
		p=1.0[a]	*p*=0.84[b]	*p*=0.50 [b]	*p*=0.14 [b]	*p*=1.0 [b]	*p*=0.19 [b]

Results are presented as median (range); n/a not applicable

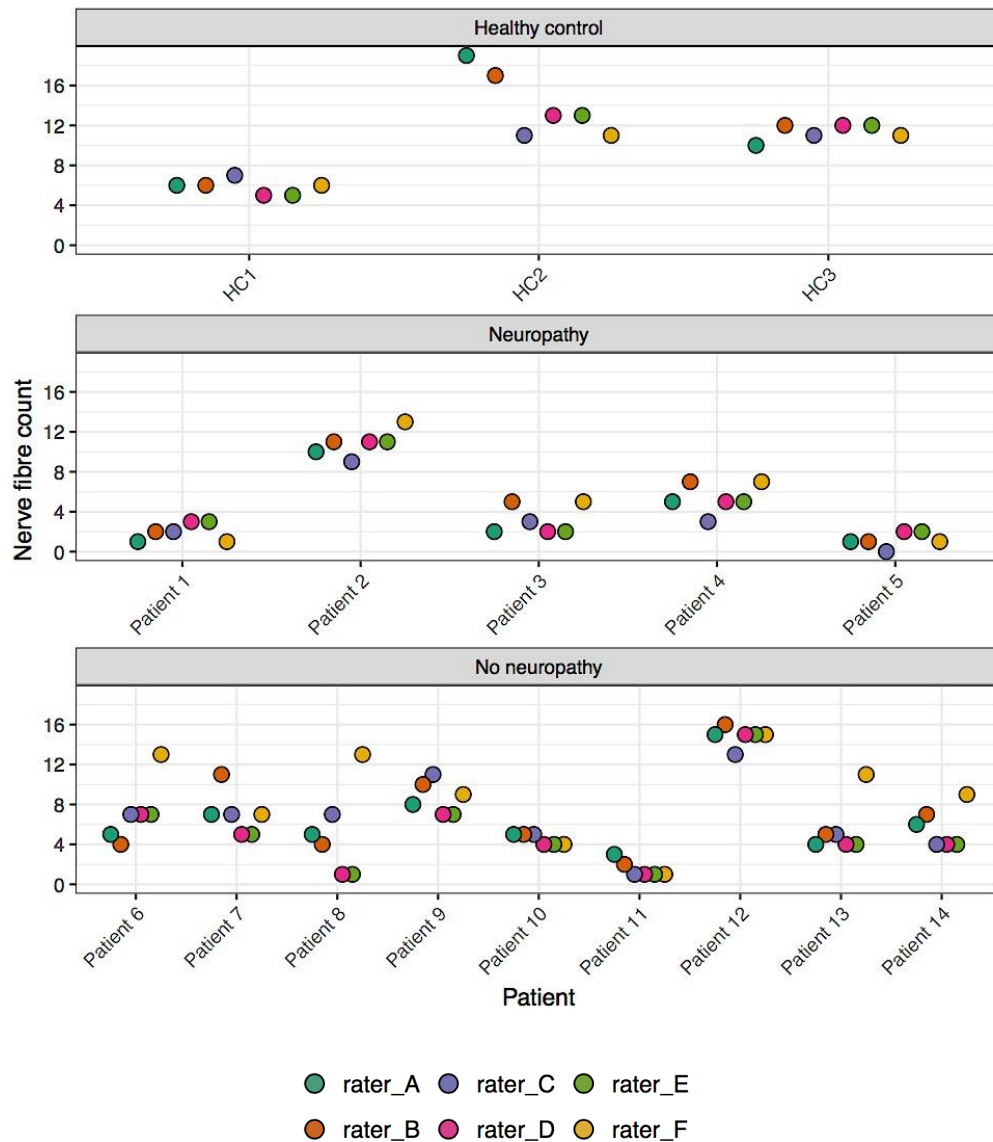[a] Fisher's exact test (HIV-SN+ *versus* HIV-SN-), [b] Mann-Whitney test (HIV-SN+ *versus* HIV-SN-)

Figure 1. Mean intraepidermal nerve fibre count for each patient as determined by each rater